

Robust model comparison tests of DAMA/LIBRA annual modulation

Aditi Krishak^{1,*}, Aisha Dantuluri^{2,†} and Shantanu Desai^{3,‡}

¹ *Department of Physics, Indian Institute of Science Education and Research, Bhopal, Madhya Pradesh 462066, India*

² *Department of Mathematics, University of California, San Diego, La Jolla, CA 92093, USA and*

³ *Department of Physics, Indian Institute of Technology, Hyderabad, Telangana-502285, India*

We evaluate the statistical significance of the DAMA/LIBRA claims for annual modulation using three independent model comparison techniques, viz frequentist, information theory, and Bayesian analysis. We fit the data from the DAMA/LIBRA experiment to both cosine and a constant model, and carry out model comparison by choosing the constant model as the null hypothesis. For the frequentist test, we invoke Wilk's theorem and calculate the significance using $\Delta\chi^2$ between the two models. For information theoretical tests, we calculate the difference in Akaike Information Criterion (AIC) and Bayesian Information criterion (BIC) between the two models. Finally, we compare the two models in a Bayesian context by calculating the Bayes factor. This is the first proof of principles application of AIC, BIC as well as Bayes factor to the DAMA data and can be easily extended to the results from other direct detection experiments looking for annual modulation.

PACS numbers:

I. INTRODUCTION

The dark matter problem [1, 2] is one of the most important vexing problems in astrophysics eluding a solution, ever since its existence was first pointed out 80-90 years ago by Oort and Zwicky [3]. The current concordance model of cosmology indicates that about 27% of universe contains cold dark matter [4]. It has been known since the 1970s that any elementary particle, which is a thermal relic from the Big-Bang and with electroweak scale interactions with ordinary matter satisfies all the properties needed for a cold dark matter candidate, such as the correct relic abundance, non-relativistic velocities at the time of decoupling, etc [5]. Therefore, such weakly interacting massive particles (hereafter, WIMPs) are the most favored dark matter candidates.

A whole slew of experiments and detection methods have been employed to experimentally detect WIMPs and measure its properties [6]. These include direct production of WIMPs at collider experiments, indirect signatures of WIMP annihilation products in cosmic rays, neutrinos, or photons, and direct detection of dark matter in underground cryogenic experiments. At the time of writing, there is no incontrovertible evidence for any smoking-gun signatures of WIMP annihilation or direct production of WIMPs (see Refs. [7–10] and references therein for most recent updates.)

Among the plethora of direct dark matter detection experiments, only one experiment (viz. the DAMA experiment in Gran Sasso) has argued for the detection of dark matter. The observational signature found by the DAMA collaboration indicative of dark matter, is the detection of annual modulation in their residual count rates,

which is based on the superposition of the motion of our Sun moving in our galaxy with respect to the Local Standard of Rest and the Earth's revolution around the Sun. It was pointed out in the 1980s [11, 12], that because of these motions, any dark matter experiment should detect a peak flux of WIMP-induced interactions around June 2 (when Earth's orbital velocity is in the same direction as that of the Sun with respect to the Galaxy) and a minimum around December 2 (when Earth's orbital velocity is in the opposite direction to that of the Sun). For more than 20 years, DAMA experiment has found such an annual modulation in their residual count rates, which has exactly the above signatures. The first phase of DAMA started in 1995. At the time of the first data release, the evidence was 3σ [13]. The statistical significance of this annual modulation has steadily increased with accumulated data taking, during the different phases of the DAMA experiment [14–18]. At the end of the first phase of the DAMA experiment (called DAMA/NaI), the statistical significance had increased to 6.3σ [14]. In the latest data release from phase 2 of the upgraded DAMA/LIBRA experiment (where the energy threshold has been lowered), the net statistical significance in the 2-6 keV energy bin, after combining data from all the phases of the experiment is 12.9σ and greater than 8σ in other energy intervals [18].

One problem with the dark matter interpretation of the above claim is that this signal has not been confirmed by any other direct detection experiment, and the entire allowed region enclosing the WIMP mass and cross-section (inferred from the DAMA annual modulation), has been ruled out by a number of other direct dark matter detection experiments [19–22]. See for example Ref. [23–25] for a recent review of all direct dark matter searches.

Although a number of particle physics, nuclear physics, and astrophysics explanations have been concocted to reconcile the incompatibility of DAMA results with other experiments (eg. [26] and references therein), none of them can satisfactorily explain all the DAMA observa-

*E-mail: aditi16@iiserb.ac.in

†E-mail: adantulu@ucsd.edu

‡E-mail: shntn05@gmail.com

tions. However, until recently none of the other direct detection dark matter experiments had used the same target as DAMA (NaI) or were sensitive to the same annual modulation signature found in DAMA; but this has been recently rectified. In 2019, two experiments ANAIS-112 and COSINE-100, which both use NaI(Tl) as the detector target released their first results. The ANAIS-112 experiment located in the Canfranc Underground Laboratory in Spain released results from modulation analysis of 1.5 years of data from 157.55 kg years exposure [27]. The COSINE-100 experiment [28] located in the Yangyang underground laboratory in South Korea released their first results using 1.7 years of data with a total exposure of 97.7 kg years. This will also be tested by other experiments, such as DM-Ice17 [29], KIMS [30], and SABRE [31].

The DAMA collaboration has calculated the statistical significance of the annual modulation claim using the frequentist test, by comparing the difference in χ^2 between the null hypothesis and the sinusoidal model [18]. Although a few other groups have done an independent statistical analysis of DAMA data [32–35], a model comparison analysis of the DAMA annual modulation claims using Bayesian or information theory methods has not been done. It is important to test the robustness of the claim using independent model comparison techniques. Such model comparison techniques are now routinely used in Cosmology to weigh the evidence for Λ CDM model versus alternatives [36–40]. This is the main goal of this work. The techniques used in this work can be easily applied to evaluate the significance of annual modulation claims of other experiments, some of which have already produced preliminary results.

The outline of this paper is as follows. In Sect. II, we provide an abridged summary of model comparison techniques. The summary of DAMA results in their latest data release paper can be found in Sect. III. Our analysis and results are described in Sect. IV. We conclude in Sect. V.

II. INTRODUCTION TO MODEL COMPARISON TECHNIQUES

In recent years a large number of both Bayesian, frequentist, and information theory based model comparison techniques (originally developed by the statistics community) have been applied to a variety of problems in astrophysics and cosmology involving hypothesis testing or comparing which of two models is favored and quantifying its statistical significance. For our purpose, we shall employ all the available techniques at our disposal to address the significance of the DAMA annual modulation claim. We briefly recap these techniques below. More details on each of these tests can be found in various reviews [36, 37, 40, 41], and proof of principles applications of some of these techniques to problems in astrophysics and cosmology can be found in Refs. [38, 42–47].

- **Frequentist Test:** This method for model comparison is sometimes also known as the Likelihood ratio test [40]. The first step in this, involves parameter estimation for a given hypothesis, usually by minimizing the χ^2 functional between the data and model. Then, based on the best-fit χ^2 between a given model and data and from the degrees of freedom, one calculates the goodness of fit for each model, given by the χ^2 probability distribution function [48]. This allows one to penalize models with complexity.

The best-fit model between the two is the one with the larger value of χ^2 goodness of fit. If the two models are nested, then from Wilk’s theorem [49], the difference in χ^2 between the two models satisfies a χ^2 distribution with degrees of freedom equal to the difference in the number of free parameters for the two hypotheses [40, 41]. Therefore, the χ^2 c.d.f. can be used to quantify the p -value of a given hypothesis. From the p -value, one usually calculates a Z -score or number of sigmas, which is the number of standard deviations that a Gaussian variable would fluctuate in one direction to give the corresponding p -value [46, 50]. This test has been used for a variety of applications in astrophysics and cosmology [42, 44, 46, 51]. We note that the DAMA collaboration also uses this test in their data release papers to assess the significance of their annual modulation claim.

- **Akaike Information Criterion:**

The Akaike Information Criterion (AIC) is used to penalize for any free parameters to avoid overfitting. AIC is an approximate minimization of Kullback-Leibler information entropy, which estimates the distance between two probability distributions [37] and is given by:

$$\text{AIC} = -2 \ln \mathcal{L}_{\max} + 2p, \quad (1)$$

where N is the total number of data points, p is the number of free parameters, and \mathcal{L} is the likelihood. A preferred model in this test is the one with the smaller value of AIC between the two hypothesis. There is no formal method to evaluate the p -value from difference in AIC between the two models [56] and usually qualitative strength of evidence rules are used [38] to estimate the relative significance of the favored model.

- **Bayesian Information Criterion:** The Bayesian Inference Criterion (BIC) is also used for penalizing the use of extra parameters and is an approximation to the Bayes factor. It is given by [36]:

$$\text{BIC} = -2 \ln \mathcal{L}_{\max} + p \ln N, \quad (2)$$

where all the parameters have the same interpretation as in Eq. 1. Similar to AIC, the model with the

smaller value of BIC is the preferred model. The significance is estimated qualitatively in the same way as for AIC.

Besides AIC and BIC, other information criterion based tests such as Takeuchi information criterion and Deviance information criterion [37] have also been proposed. But their computation as well as interpretation is not straightforward, and hence we do not implement them in this work.

- **Bayesian Model Selection:** Apart from the information theory-based techniques such as AIC and BIC, Bayesian model comparison techniques [39] have also been extensively used for model comparison in astrophysics and cosmology [39, 42, 43, 52]. The key quantity, which needs to be computed to compare two models (M_1 and M_2) is the Bayesian odds ratio, given by:

$$O_{21} = \frac{P(M_2|D)}{P(M_1|D)}, \quad (3)$$

where $P(M_2|D)$ is the posterior probability for M_2 given data D , and similarly for $P(M_1|D)$. The posterior probability for a general model M is given by

$$P(M|D) = \frac{P(D|M)P(M)}{P(D)}, \quad (4)$$

where $P(M)$ is the prior probability for the model M , $P(D)$ is the probability for the data D and $P(D|M)$ is the marginal likelihood or Bayesian evidence for model M and it quantifies the probability that the data D would be observed if the model M were the correct model. $P(D|M)$ is given by:

$$P(D|M) = \int P(D|M, \theta)P(\theta|M)d\theta, \quad (5)$$

where θ is a vector of parameters, which parametrizes the model M . If the prior probabilities of the two models are equal, the odds ratio can be written as:

$$B_{21} = \frac{\int P(D|M_2, \theta_2)P(\theta_2)d\theta_2}{\int P(D|M_1, \theta_1)P(\theta_1)d\theta_1}, \quad (6)$$

The quantity B_{21} in Eq. 6 is known as Bayes factor. We shall compute this quantity in order to obtain a Bayesian estimate of the statistical significance.

Unlike the frequentist model-comparison technique, there is no quantitative way to rank between two models. However, similar to AIC and BIC, a qualitative criterion based on Jeffreys scale is used to interpret the odds ratio or Bayes factor [39, 48]. A value of > 10 represents strong evidence in favor of M_2 , and a value of > 100 represents decisive evidence [39, 48].

III. SUMMARY OF DAMA/LIBRA PHASE2 RESULTS

Here, we provide a succinct summary of the key results in the latest data release paper from DAMA/LIBRA [18], which we later try to reproduce. For more details, the reader can consult Ref. [18].

The total data presented in Ref. [18] for 1-3 keV and 1-6 keV corresponds to six annual cycles of the DAMA/LIBRA phase II, with a total exposure of 1.13 ton year. The data in the 2-6 keV energy bin corresponds to the DAMA/LIBRA phase II data combined with data from DAMA/NaI and DAMA/LIBRA phase I (collected over 14 annual cycles), with a total exposure of 2.46 ton year. In previous DAMA papers [14–17] containing a combination of data from phase I of DAMA/LIBRA experiment as well as DAMA/NaI, single hit rates were also presented in the 2-4 keV, 2-5 keV, and 2-6 keV energy intervals.

The DAMA Collaboration looks for an annual modulation signature indicative of a dark matter signal, which must satisfy some basic characteristic such as a period of one year, a phase peaked roughly around June 2nd, occurring only in single-hit events, and the modulation amplitude having at most 7% of the DC amplitude [18]. The single-hit residual rates in DAMA/LIBRA phase 2 have been fit to the following cosine function

$$H_1(x) = A \cos \omega(x - t_0), \quad (7)$$

where $\omega = \frac{2\pi}{T}$ corresponding to period T . Their best-fit values are given by $T \sim 1$ year, $t_0 \sim 152.5$ days (at around June 2), and $A \sim 0.01$ cpd/kg/keV. The reduced χ^2 for all the fits are close to 1 and can be found in Table 1 of Ref. [18]. The statistical significance of this annual modulation corresponds to a Z -score of 8.0σ , 9.6σ , and 8.7σ in 1-3 keV, 1-6 keV, and 2-6 keV energy intervals respectively. When the 2-6 keV data is combined with data from DAMA/NaI and phase 1 of DAMA/LIBRA, the significance gets enhanced to 12.9σ . In the 2012 data release from DAMA/LIBRA, the significance of annual modulation in 2-4 and 2-5 keV intervals was 7.6σ .

IV. ANALYSIS AND RESULTS

For our analysis, the data and the associated errors in the plots (from Ref. [18]) in each energy interval has been digitized [57]. The published data consists of single-hit residual rates in three different energy intervals. Each data point consists of experimental errors (presumably both statistical and systematic) in the residual rates, as well as the associated time widths as errors in the independent variable. The abscissa values range from 6200 to 8300 days for 1-3 and 1-6 keV energy intervals and from 3000 to 8300 days for 2-6 keV interval(cf. Figs. 2 and 3 in Ref. [18]).

In order to independently evaluate the significance of the apparent annual modulation present in the signal, we

use both a constant function, given by

$$H_0(x) = k, \quad (8)$$

and the cosine model in Eqn. 7 as two different models, and compare the best fits for both of them. Initially, we estimate the best-fit parameters for both these hypotheses. This is the first step for model comparison. The constant function is then considered as the null hypothesis and model comparison is carried out accordingly.

A. Parameter Estimation

The first step in model comparison involves estimating the best-fit parameters of a given model. For this purpose, we construct a χ^2 function between the data and a given model. We also include the errors in the time bin. Although, no details of the χ^2 functional used for minimization is provided in Ref. [18] or in earlier papers, most likely their χ^2 does not include the errors in the abscissa. To incorporate the error in the independent time variable, we follow the method of Ref. [53] and the total error (σ_t) is given by:

$$\sigma_t = \sqrt{\sigma_H^2 + \sigma_x^2 \left(\frac{\partial H}{\partial x} \right)^2}, \quad (9)$$

where σ_H is the error in residual rate (obtained by digitization of the relevant plots in Ref. [18]), σ_x is the error in time variable and $\frac{\partial H}{\partial x}$ is obtained from Eq. 7. We assume that the error bars provided by DAMA/LIBRA collaboration are robust and all systematic terms have been included, and we don't need to fit for unknown systematic error terms (for eg. Ref [51] in the context of periodicity in measurements of Newton's constant). We also assume that the amplitude A in Eqn. 7 does not vary with time. Time-dependence of A is explored in Ref. [33]. The χ^2 functional is then given by:

$$\chi^2 = \sum_{i=1}^N \left(\frac{y_i - H(x)}{\sigma_t} \right)^2 \quad (10)$$

where $H(x)$ is defined in Eq. 7 and y_i denote the residual single-hit DAMA rates in each time bin i . For finding the minimum value of χ^2 , we have kept free all the three parameters of the cosine function.

For each of the given sets of data in the 2-4, 2-5, 2-6, 1-6, 2-6 keV range, the data is fit to both the hypotheses by minimizing the χ^2 in Eq. 10 to obtain the best-fit parameters. The parameters obtained for all the energy ranges are displayed in Table I for the cosine and also the constant models. The values of parameters obtained for the cosine model, $H_1(x)$ more or less agree with those found in Ref. [18] as those obtained by the DAMA collaboration. Fig. 1 presents the best fit constant value as obtained for $H_0(x)$ for each energy range, along with the best fit cosine waves obtained, in comparison to the

cosine wave with the best fit parameters presented by the DAMA collaboration [17].

From the figures, we see that the cosine model appears to fit the data very well for all the five sets of data. To quantify this goodness of fit, we calculate the value of χ^2/DOF , and additionally the value of χ^2 probability as defined in Section II, hereafter denoted as GOF for goodness of fit. It is expected that for reasonably good fits, the value of χ^2/DOF will be close to 1. The values of χ^2/DOF and GOF are indicated in Table II. We see that the values of χ^2/DOF are much closer to 1 for the cosine model than for the constant model. Additionally, the GOF values for the cosine model are of the order of 10^{-2} , whereas for the constant model the values are in the order of 10^{-6} . Thus, we can reasonably conclude that the cosine model provides a better fit to the data. Further, the time period of the observed fit is very close to 1 year, and the phase offset, t_0 is comparable to the required 152.5 days. Thus, the frequentist test strongly supports annual modulation.

B. Frequentist Model Comparison

As noted in Sect. II, it is possible to take advantage of the fact that the constant model is nested within the cosine model (when $A = 0$), and apply Wilk's theorem to evaluate the statistical significance of the cosine model in comparison to the null hypothesis. Thus, the difference in χ^2 between the constant and the cosine models follows a χ^2 distribution with $\text{DOF} = 2$ [40, 41]. From the distributions obtained, we calculate the p -value of the cosine model for each set of data separately, from the cumulative distribution of the χ^2 functional. The p -values obtained are depicted alongside the difference in χ^2 values in Table III. The p -value can be interpreted as the probability that we would see data that favours the cosine model by chance, given that the null hypothesis is true. Thus, the low values of the p -value indicate that the cosine model should be favored over the constant model. For each of the energy ranges, the corresponding significance (or Z -score) is calculated [46, 50]. Its value is given alongside the p -value. These can be found in Table III. We note that the significance values are comparable (within $\pm 1\sigma$) to the values indicated in the DAMA/LIBRA findings, presented in Refs. [17, 18].

C. Information Criteria

Subsequently, we proceed to calculate the difference in AIC and BIC values between the null hypothesis and the cosine model, where the values are calculated using Eqns. 1 and 2. In general, the model with the smaller AIC and BIC values is preferred. The ΔAIC and ΔBIC values can be found in Table III, where the cosine model has the smaller value. From the difference in AIC and BIC values, we evaluate the significance using the qualitative

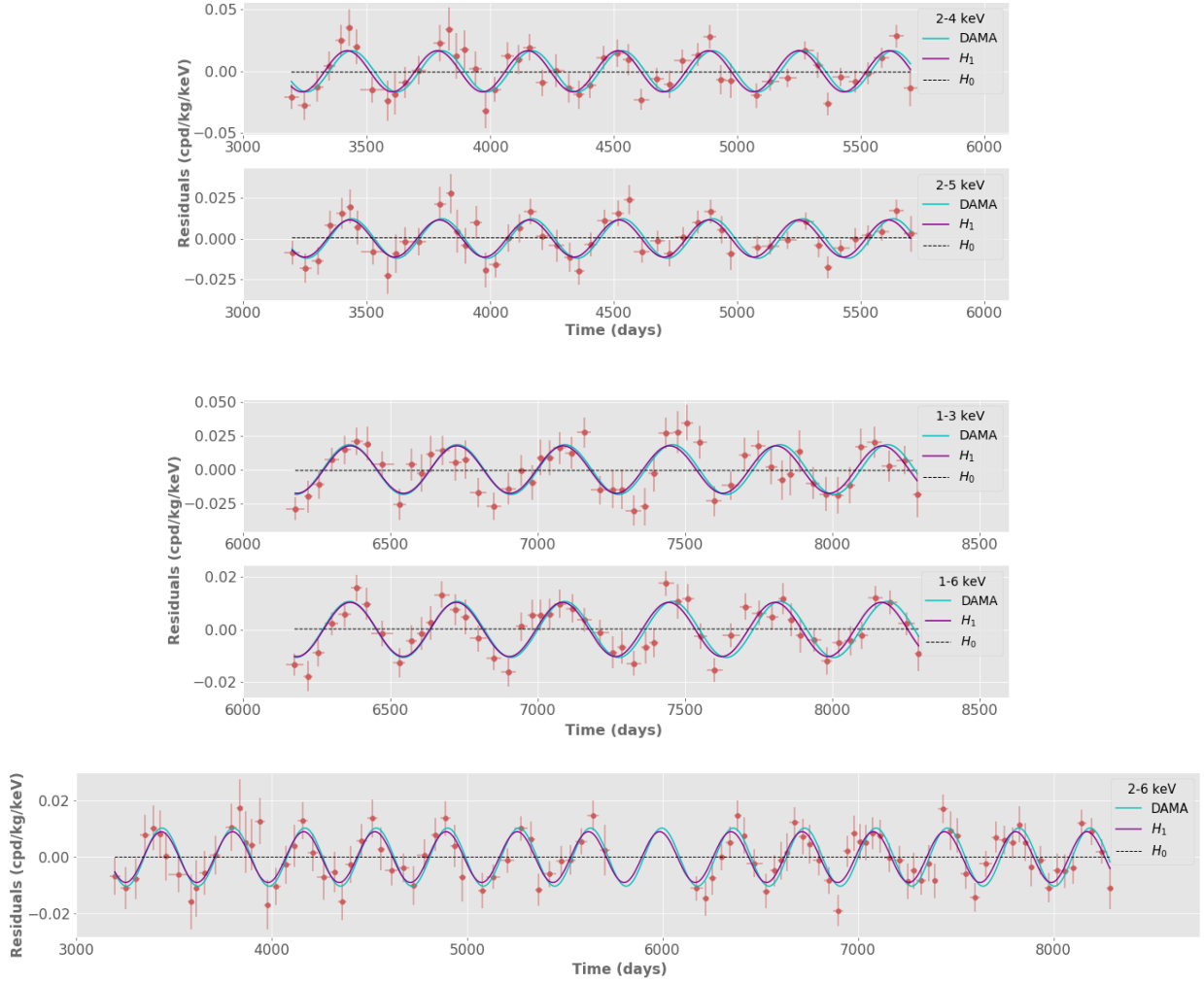


FIG. 1: The DAMA data points (red) in each energy range, namely 2-4 keV, 2-5 keV, 1-3 keV, 1-6 keV, and 2-6 keV, are overlaid with both the corresponding calculated fits of $H_1(x)$ (Eq. 7) to the data, as well as the fits the DAMA/LIBRA collaboration calculated, as depicted in the first set of values in Table 1 of Ref. [18]. The sinusoidal fit calculated by this work is depicted in purple while that calculated by the DAMA/LIBRA collaboration is shown in cyan. The calculated fit for $H_0(x)$ is also shown.

Energy Interval	H_1			H_0
	A (cpd/kg/keV)	ω (radians/day)	t_0 (days)	k (cpd/kg/keV)
2012 data				
2-4 keV	0.0167	0.0172	131.69	-6.42×10^{-4}
2-5 keV	0.0115	0.0173	161.84	4.20×10^{-4}
2018 data				
1-3 keV	0.0175	0.0174	224.17	-6.41×10^{-4}
1-6 keV	0.0102	0.0174	234.13	1.50×10^{-4}
2012 + 2018 data				
2-6 keV	0.0090	0.0172	156.67	-2.16×10^{-5}

TABLE I: Best-fit values for different parameters of the cosine model (cf. Eqn. 7) as well as the constant model (cf. Eqn. 8) to the DAMA data points in different energy intervals.

Model	2012 data				2018 data				2012 + 2018 data	
	2-4 keV		2-5 keV		1-3 keV		1-6 keV		2-6 keV	
	Cosine	Constant	Cosine	Constant	Cosine	Constant	Cosine	Constant	Cosine	Constant
χ^2/DOF	35.5/47	110.5/49	32.4/47	99.8/49	43.7/49	110.4/51	38.0/49	153.6/51	59.2/99	198.3/101
GOF	0.023	3.55×10^{-7}	0.014	6.85×10^{-6}	0.039	8.08×10^{-7}	0.025	1.13×10^{-12}	1.82×10^{-4}	6.57×10^{-9}

TABLE II: Summary of best-fit χ^2 per degrees of freedom, GOF (obtained using the χ^2 p.d.f for the cosine and constant model) for the different energy intervals. The corresponding values for these by the DAMA/LIBRA collaboration can be found in Ref. [18] for the 2018 data and in Tables 2 and 3 for the 2012 data in Ref. [17].

“strength of evidence rules” provided in Ref. [38]. As all the values of ΔAIC and ΔBIC are in the range of 50-100, they provide *very strong evidence* against the null hypothesis, according to the aforementioned scale.

D. Bayesian Analysis

Finally, we proceed to calculate the Bayesian odds ratio B_{21} for the M_2 model in comparison to the M_1 hypothesis. For this purpose, we consider the null hypothesis to be M_1 and the cosine model to be M_2 . Each set of points in a given energy range is separately considered as data D , and B_{21} is calculated for each energy range, namely 2-4 keV, 2-5 keV, 1-3 keV, 1-6 keV, and 2-6 keV.

We initially need to calculate the Bayesian evidence for each of the two models. The first step in the calculation of Bayesian evidence is the likelihood of the data, given the model and a set of parameters, and for this purpose we use a Gaussian likelihood

$$P(D|M, \theta) = \prod_{i=1}^N \frac{1}{\sigma_t \sqrt{2\pi}} \exp \left[-\frac{1}{2} \left(\frac{y_i - H(x)}{\sigma_t} \right)^2 \right], \quad (11)$$

where σ_t is the total error defined in Eq. 9, y_i denote the DAMA data and $H(x)$ represents the model, which in this case is either the constant or sinusoidal model.

The Bayesian priors chosen are the constant k and the amplitude A uniform over $[0, A_{max}]$ (where A_{max} is the maximum absolute value of the residual rate in the particular data set in consideration, with the mean of the A_{max} values from the five data sets being 0.0270 cpd/kg/keV), ω uniform over $[0, 2\pi/365.25]$ and the phase ωt_0 uniform over $[0, 2\pi]$. To calculate the Bayesian evidence for both the hypotheses, we used the **Nestle** package in **Python** [58], which uses the nested sampling algorithm [54, 55].

The Bayes factor is given by the ratio of Bayesian evidence for the cosine and constant model hypothesis. The Bayes factors for different combinations of datasets and energy intervals are summarized in Table III. We interpret the Bayes factor using the Jeffrey’s Scale [39]. As the values of Bayes factor are well above 100 for all data sets, we conclude that they provide *decisive evidence* against the null hypothesis.

V. CONCLUSIONS

The DAMA experiment, which looks for direct detection of dark matter, has found evidence for annual modulation for more than 20 years, with all the right characteristics to be caused by galactic dark matter scattering. In their latest data release paper from phase 2 of their upgraded experiment (called DAMA/LIBRA) [18], the statistical significance ranges from 8σ and 12.9σ , depending on the energy intervals and durations [18].

This statistical significance has been evaluated using a frequentist technique, which involves comparing the difference in χ^2 between the null hypothesis and sinusoidal model. From this difference, a p -value can be calculated using Wilk’s theorem, which is then converted to a Z -score or significance, in terms of number of sigmas.

In this work, we independently assess the DAMA claim for annual modulation using the same frequentist model comparison technique, by including the errors in the independent time-variable. Furthermore, we use model comparison tests from information theory and Bayesian analysis, which are routinely used in Cosmology. For the information theory tests, we used the Akaike Information Criterion and Bayesian Information Criterion to evaluate the significance. From the difference, the significance was evaluated using qualitative strength of evidence rules. For Bayesian model comparison, we calculated the marginal likelihood or Bayesian evidence for both the hypotheses. For this purpose, we assumed uniform priors on all the models. We then calculated the Bayes factor from the ratio of the marginal likelihood and used Jeffrey’s scale to evaluate the significance.

A tabular summary of all our model comparison tests can be found in Table III. The Bayesian and information theoretical comparison tests also point to very strong evidence for annual modulation and agree with the frequentist tests.

This is the first proof of principles application of information theoretic and Bayesian model comparison techniques to evaluate the annual modulation claim in DAMA. The same technique can be easily applied to other direct detection experiments looking for annual modulation such as COSINE-100, ANAIS-112, DM-Ice17, SABRE, KIMS, etc.

All our analysis codes and data to reproduce these results are available online at <https://github.com/>

Energy interval	$\Delta\chi^2$	p -value	Z -score	ΔAIC	ΔBIC	Bayes Factor
2012 data						
2-4 keV	75.0	5.18×10^{-17}	8.3σ	59.68	55.85	4.30×10^{10}
2-5 keV	67.3	2.37×10^{-15}	7.8σ	53.23	49.41	3.29×10^8
2018 data						
1-3 keV	66.8	3.16×10^{-15}	7.8σ	55.26	51.35	9.46×10^9
1-6 keV	115.5	8.17×10^{-26}	10.4σ	99.46	95.56	1.26×10^{18}
2012 + 2018 data						
2-6 keV	139.2	6.02×10^{-31}	11.5σ	117.17	111.92	2.82×10^{17}

TABLE III: Summary of model comparison results for the sinusoidal variation to the DAMA data compared to the constant fit as the null hypothesis, using all three model comparison techniques. The first two columns depict the $\Delta\chi^2$ value between the constant fit 8 and the cosine model 7 and the p -value obtained using Wilk's theorem. The third column indicates the Z -score. The corresponding Z -scores found by the DAMA collaboration can be found in Table 2 of Ref. [18] for the 2018 data and in Table 4 of Ref. [17]. The next two columns indicate the difference in AIC and BIC between the two models. Finally, the last column shows the Bayes factor between the two models. As we can see, the sinusoidal model is decisively favored over the constant model using all the three techniques.

aditikrishak/DAMA_Model_Comparison.

-
- [1] G. Jungman, M. Kamionkowski, K. Griest, Physics Reports **267**, 195 (1996). DOI 10.1016/0370-1573(95)00058-5
- [2] G. Bertone, D. Hooper, J. Silk, Physics Reports **405**, 279 (2005). DOI 10.1016/j.physrep.2004.08.031
- [3] G. Bertone, D. Hooper, Reviews of Modern Physics **90**(4), 045002 (2018). DOI 10.1103/RevModPhys.90.045002
- [4] P.A.R. Ade, et al., Astron. Astrophys. **594**, A13 (2016). DOI 10.1051/0004-6361/201525830
- [5] B.W. Lee, S. Weinberg, Physical Review Letters **39**, 165 (1977). DOI 10.1103/PhysRevLett.39.165
- [6] D. Bauer, J. Buckley, M. Cahill-Rowley, R. Cotta, A. Drlica-Wagner, J.L. Feng, S. Funk, J. Hewett, D. Hooper, A. Ismail, M. Kaplinghat, A. Kusenko, K. Matchev, D. McKinsey, T. Rizzo, W. Shepherd, T.M.P. Tait, A.M. Wijangco, M. Wood, Physics of the Dark Universe **7**, 16 (2015). DOI 10.1016/j.dark.2015.04.001
- [7] S. Desai, et al., Phys. Rev. **D70**, 083523 (2004). DOI 10.1103/PhysRevD.70.083523, 10.1103/PhysRevD.70.109901. [Erratum: Phys. Rev.D70,109901(2004)]
- [8] M. Cirelli, Pramana **79**, 1021 (2012). DOI 10.1007/s12043-012-0419-x
- [9] M. Klasen, M. Pohl, G. Sigl, Progress in Particle and Nuclear Physics **85**, 1 (2015). DOI 10.1016/j.ppnp.2015.07.001
- [10] M. Felcini, arXiv e-prints arXiv:1809.06341 (2018)
- [11] A.K. Drukier, K. Freese, D.N. Spergel, Phys. Rev. D **33**, 3495 (1986). DOI 10.1103/PhysRevD.33.3495
- [12] K. Freese, J. Frieman, A. Gould, Phys. Rev. D **37**, 3388 (1988). DOI 10.1103/PhysRevD.37.3388
- [13] R. Bernabei, P. Belli, R. Cerulli, F. Montecchia, M. Amato, G. Ignesti, A. Incicchitti, D. Prosperi, C.J. Dai, H.L. He, H.H. Kuang, J.M. Ma, Nuclear Physics B Proceedings Supplements **87**, 67 (2000). DOI 10.1016/S0920-5632(00)00633-2
- [14] R. Bernabei, P. Belli, F. Cappella, R. Cerulli, F. Montecchia, F. Nozzoli, A. Incicchitti, D. Prosperi, C.J. Dai, H.H. Kuang, J.M. Ma, Z.P. Ye, Nuovo Cimento Rivista Serie **26**(1), 1 (2003)
- [15] R. Bernabei, P. Belli, F. Cappella, R. Cerulli, C.J. Dai, A. D'Angelo, H.L. He, A. Incicchitti, H.H. Kuang, J.M. Ma, F. Montecchia, F. Nozzoli, D. Prosperi, X.D. Sheng, Z.P. Ye, European Physical Journal C **56**, 333 (2008). DOI 10.1140/epjc/s10052-008-0662-y
- [16] R. Bernabei, P. Belli, F. Cappella, R. Cerulli, C.J. Dai, A. D'Angelo, H.L. He, A. Incicchitti, H.H. Kuang, X.H. Ma, F. Montecchia, F. Nozzoli, D. Prosperi, X.D. Sheng, R.G. Wang, Z.P. Ye, European Physical Journal C **67**, 39 (2010). DOI 10.1140/epjc/s10052-010-1303-9
- [17] R. Bernabei, et al., Eur. Phys. J. **C73**, 2648 (2013). DOI 10.1140/epjc/s10052-013-2648-7
- [18] R. Bernabei, P. Belli, A. Bussolotti, F. Cappella, V. Caracciolo, R. Cerulli, C.J. Dai, A. d'Angelo, A. Di Marco, H.L. He, A. Incicchitti, X.H. Ma, A. Mattei, V. Merlo, F. Montecchia, X.D. Sheng, Z.P. Ye, Universe **4**(11), 116 (2018). DOI 10.3390/universe4110116
- [19] D.S. Akerib, et al., Phys. Rev. Lett. **118**(2), 021303 (2017). DOI 10.1103/PhysRevLett.118.021303
- [20] X. Cui, et al., Phys. Rev. Lett. **119**(18), 181302 (2017). DOI 10.1103/PhysRevLett.119.181302
- [21] E. Aprile, et al., Phys. Rev. Lett. **121**(11), 111302 (2018). DOI 10.1103/PhysRevLett.121.111302
- [22] H. Jiang, et al., Phys. Rev. Lett. **120**(24), 241301 (2018). DOI 10.1103/PhysRevLett.120.241301
- [23] T. Marrodán Undagoitia, L. Rauch, Journal of Physics G Nuclear Physics **43**(1), 013001 (2016). DOI 10.1088/0954-3899/43/1/013001
- [24] A. Bottino, arXiv e-prints arXiv:1904.05711 (2019)
- [25] M. Schumann, arXiv e-prints arXiv:1903.03026 (2019)
- [26] C. Savage, G. Gelmini, P. Gondolo, K. Freese, JCAP

- 0904**, 010 (2009). DOI 10.1088/1475-7516/2009/04/010
- [27] J. Amaré, S. Cebrián, I. Coarasa, C. Cuesta, E. García, M. Martínez, M.A. Oliván, Y. Ortigoza, A. Ortiz de Solórzano, J. Puimedón, arXiv e-prints arXiv:1903.03973 (2019)
- [28] COSINE-100 Collaboration, :, G. Adhikari, P. Adhikari, E. Barbosa de Souza, N. Carlin, S. Choi, M. Djamel, A.C. Ezeribe, C. Ha, arXiv e-prints arXiv:1903.10098 (2019)
- [29] E. Barbosa de Souza, et al., Phys. Rev. **D95**(3), 032006 (2017). DOI 10.1103/PhysRevD.95.032006
- [30] K.W. Kim, G. Adhikari, P. Adhikari, S. Choi, C. Ha, I.S. Hahn, E.J. Jeon, H.W. Joo, W.G. Kang, H.J. Kim, Journal of High Energy Physics **2019**(3), 194 (2019). DOI 10.1007/JHEP03(2019)194
- [31] M. Antonello, E. Barberio, T. Baroncelli, J. Benziger, L.J. Bignell, I. Bolognino, F. Calaprice, S. Copello, D. D'Angelo, G. D'Imperio, European Physical Journal C **79**(4), 363 (2019). DOI 10.1140/epjc/s10052-019-6860-y
- [32] P.A. Sturrock, E. Fischbach, J.T. Gruenwal, D. Javorsek, II, J.H. Jenkins, R.F. Lang, R.H. Lee, J. Nistor, J. Scargle, ArXiv e-prints (2013)
- [33] C. Kelso, C. Savage, P. Sandick, K. Freese, P. Gondolo, Eur. Phys. J. **C78**(3), 223 (2018). DOI 10.1140/epjc/s10052-018-5685-4
- [34] S. Baum, K. Freese, C. Kelso, Phys. Lett. **B789**, 262 (2019). DOI 10.1016/j.physletb.2018.12.036
- [35] F. Kahlhoefer, F. Reindl, K. Schffner, K. Schmidt-Hoberg, S. Wild, JCAP **1805**(05), 074 (2018). DOI 10.1088/1475-7516/2018/05/074
- [36] A.R. Liddle, Mon. Not. R. Astron. Soc. **351**, L49 (2004). DOI 10.1111/j.1365-2966.2004.08033.x
- [37] A.R. Liddle, Mon. Not. R. Astron. Soc. **377**, L74 (2007). DOI 10.1111/j.1745-3933.2007.00306.x
- [38] K. Shi, Y.F. Huang, T. Lu, Mon. Not. R. Astron. Soc. **426**, 2452 (2012). DOI 10.1111/j.1365-2966.2012.21784.x
- [39] R. Trotta, arXiv e-prints arXiv:1701.01467 (2017)
- [40] M. Kerscher, J. Weller, arXiv e-prints arXiv:1901.07726 (2019)
- [41] L. Lyons, arXiv e-prints arXiv:1607.03549 (2016)
- [42] D.L. Shafer, Phys. Rev. D **91**(10), 103516 (2015). DOI 10.1103/PhysRevD.91.103516
- [43] A. Heavens, Y. Fantaye, E. Sellentin, H. Eggers, Z. Hoseinie, S. Kroon, A. Mootooyaloo, Physical Review Letters **119**(10), 101301 (2017). DOI 10.1103/PhysRevLett.119.101301
- [44] S. Kulkarni, S. Desai, Astrophys. and Space Science **362**, 70 (2017). DOI 10.1007/s10509-017-3047-6
- [45] S. Desai, D.W. Liu, Astroparticle Physics **82**, 86 (2016). DOI 10.1016/j.astropartphys.2016.06.004
- [46] S. Ganguly, S. Desai, Astroparticle Physics **94**, 17 (2017). DOI 10.1016/j.astropartphys.2017.07.003
- [47] D. Keitel, Mon. Not. R. Astron. Soc. **485**(2), 1665 (2019). DOI 10.1093/mnras/stz358
- [48] Ž. Ivezić, A. Connolly, J. Vanderplas, A. Gray, *Statistics, Data Mining and Machine Learning in Astronomy* (Princeton University Press, 2014)
- [49] S.S. Wilks, Annals Math. Statist. **9**(1), 60 (1938). DOI 10.1214/aoms/1177732360
- [50] G. Cowan, arXiv e-prints arXiv:1307.2487 (2013)
- [51] S. Desai, EPL (Europhysics Letters) **115**, 20006 (2016). DOI 10.1209/0295-5075/115/20006
- [52] M. Pitkin, EPL (Europhysics Letters) **111**(3), 30002 (2015). DOI 10.1209/0295-5075/111/30002
- [53] B.J. Weiner, C.N.A. Willmer, S.M. Faber, J. Harker, S.A. Kassin, A.C. Phillips, J. Melbourne, A.J. Metevier, N.P. Vogt, D.C. Koo, Astrophys. J. **653**, 1049 (2006). DOI 10.1086/508922
- [54] F. Feroz, M.P. Hobson, M. Bridges, Mon. Not. R. Astron. Soc. **398**(4), 1601 (2009). DOI 10.1111/j.1365-2966.2009.14548.x
- [55] P. Mukherjee, D. Parkinson, A.R. Liddle, Astrophys. J. **638**(2), L51 (2006). DOI 10.1086/501068
- [56] See however Ref. [42], which posits a significance based on $\exp(-\Delta AIC/2)$
- [57] The raw DAMA data presented in their papers is not publicly available to the best of our knowledge
- [58] See <http://github.com/kbarbary/nestle>